RSC Chemical Biology

ROYAL SOCIETY OF CHEMISTRY

PAPER

View Article Online
View Journal | View Issue

Cite this: *RSC Chem. Biol.*, 2022, 3, 250

Phosphorylated resveratrol as a protein aggregation suppressor *in vitro* and *in vivo*†

Johannes Mehringer,[a] Juan Antonio Navarro,[b] Didier Touraud,[a] Stephan Schneuwly[c] and Werner Kunz *[a]

Received 22nd November 2021,
Accepted 26th December 2021

DOI: 10.1039/d1cb00220a

rsc.li/rsc-chembio

The stability of proteins in solution poses a great challenge for both technical applications and molecular biology, including neurodegenerative diseases. In this work, a phosphorylated resveratrol material was examined for its anti-aggregation properties *in vitro* and *in vivo*. Here, an anti-fibrillation effect could be measured for amyloid beta and human insulin *in vitro* and general anti-aggregation properties for crude chicken egg white in solution. Using a drosophila fly model for the overexpression of amyloid beta protein, changes in physiological protein aggregation and improved locomotor abilities could be observed in the presence of dietary phosphorylated resveratrol.

Introduction

Protein aggregation plays an important role not only for medical reasons as in conformational diseases (proteopathy), but also for a variety of technical applications. Hence, compounds that can suppress misfolding and subsequent aggregation of proteins have a wide field of application.[1,2]

In a simplified model, one can discriminate between three conceptually different types of aggregation: one that forms from native protein that has surpassed its solubility or is complexed by bridging ions (*e.g.* multivalent salts) to form loose aggregates, that can be re-dispersed by changing the solvent environment. The second type of aggregation is preceded by a denaturation step where the peptide-chain starts to unfold, exposing hydrophobic patches normally buried inside the protein.[3,4] This will lead to a virtually irreversible aggregation, which is solidified by inter-molecular crosslinking (*e.g.* disulfide shuffling).[4] Additionally, other non-native aggregation forms such as fibrillation are known. Here, proteins (often without well-defined native ternary structure) assume a beta-sheet rich conformation, that will eventually lead to the formation of oligomer or fiber-like aggregates. These non-native aggregates can be toxic and are associated with a variety of conformational diseases such as glaucoma, amyloidosis, Alzheimer's and Parkinson's disease.[5–7] While Alzheimer's disease is not fully understood yet, it becomes apparent that excessive accumulation of amyloid beta protein inside the brain (especially in oligomeric form) contributes to synaptic and mitochondrial failure, oxidative stress and inflammation. All of which manifests in cognitive decline and neuronal loss which is typically observed in Alzheimer's patients.[8]

The compound examined in this paper is a phosphorylated derivative of *trans*-resveratrol, a well-known polyphenolic substance of natural origin. *Trans*-Resveratrol has been reported in the past to potentially have positive effects on human health regarding obesity, diabetes, various forms of cancer, Alzheimer's and cardiovascular diseases besides others.[9] The underlying mechanisms are not entirely clear, but a variety of effects have been suggested in the past. As an anti-oxidant, *trans*-resveratrol is assumed to reduce oxidative stress in cells by radical-scavenging,[10,11] but it was also shown that it can directly interact with gene expression.[12,13] Concerning conformational diseases, the effect of *trans*-resveratrol is in part exerted by preventing the fibrillation of pathogenic proteins such as amyloid beta.[14–16] This effect is thought to be owed to π–π interactions,[17] besides other binding modes relying on hydroxyl groups.[16]

The solubility of *trans*-resveratrol is, however, very low ($\lesssim$300 μM with sonication),[18] making formulations that achieve high bioavailability very challenging.[19] To this end, a variety of delivery systems and derivatives (*i.e.* prodrugs) have been devised to approach this issue.[20] By introducing phosphate groups to the molecular structure through esterification of the hydroxy-groups, the compound becomes highly water soluble and can also exert specific ion effects. Hence, phosphorylated resveratrol (PR) can affect proteins (*in vitro* and *in vivo*) through the special interactions of its extended π-system, while potentially featuring a better (bio)availability.

[a] *Institute of Physical and Theoretical Chemistry, University of Regensburg, Germany. E-mail: Werner.Kunz@ur.de*
[b] *INCLIVA Biomedical Research Institute, Valencia, Spain*
[c] *Institute of Zoology, University of Regensburg, Germany*

† Electronic supplementary information (ESI) available. See DOI: 10.1039/d1cb00220a

Experimental

Materials

Chemicals. Thioflavine T and disperse red 13 (95%), were purchased from Sigma-Aldrich. The acetonitril (99.5%) was acquired from VWR Chemicals. The phosphorylated resveratrol (PR, 60–85%) was obtained from Ajinomoto OmniChem as a free sample and was marketed as ''resveratrol triphosphate trisodium salt''. The pH was adjusted using HCl (1 N, VWR Chemicals) and NaOH (1 N, Roth). Deionized water (Millipore quality) with a resistivity of 18 MΩ cm was used. The fly food was prepared from formula 4-24 drosophila instant medium by Schlüter Biologie.

Polypeptides. Amyloid β protein fragment 1-42 (≥95%) and human insulin solution (BioXtra) were obtained from Sigma-Aldrich. Egg white was prepared from fresh chicken eggs bought in local supermarkets.

Immunostaining. Rabbit anti-oligomer (A11) by Invitrogen, rabbit anti-amyloid fibrils OC (AB2286) by EMD Millipore Corp. and mouse anti-aβ 1-16 (6E10) by BioLegend were used as primary antibodies in combination with goat anti-mouse or anti-rabbit alexa fluor 555 by Thermo Fisher as secondary antibodies for immunostaining. Specimen mounting was done using VECTASHIELD by Vector laboratories. Fly fixation was done using PFA (>95%) by Merck and Triton × 100 by Roth.

qPCR reagents. qPCR was performed using SYBR ORA qPCR green ROX by highQu, Quanti Tect Reverse Transcription Kit by Qiagen, DEPC water (≥97%) by Roth, 2-propanol (100%) by VWR and TRIZOL (ambion) by life technologies. The primer RNAs used were ABpBACFW, ABpBACRV, 2xABFW, 2xABRV, RP49RTFw and RP49RTRv by Invitrogen.

Methods

Disperse red 13

Sample solutions were prepared in their respective concentrations in MilliQ. Then 2 mL of each solution were added to 10 mg of Disperse Red 13 and stirred in the dark for 24 h. After that, the solutions were filtered by means of a 200 nm syringe filter and measured for absorbance at 503 nm using a PerkinElmer Lambda 19 Spectrophotometer. Samples exceeding 1.5 absorbance were diluted accordingly. All measurements were done in duplicates and the results averaged.

Turbidimetry

Turbidity was measured at 488 nm by means of a photometer. For temperature scans, 20 mL of the sample solution was heated in a water bath at a constant rate of 1 K min^{-1}. At appropriate temperature increments, a small volume was retrieved and subjected to absorbance/transmission measurement. All measurements were done in duplicates or triplicates and the results averaged.

Thioflavine T assay (amyloid)

The Thioflavine T assay was performed in black half area 96 well plates utilizing a nano M Multimode plate reader by Tecan. For this, 70 μL of sample (or background) was mixed with 10 μL of 0.11 mM Amyloid42 in 50/50 Acetontril/Water (or blank) and incubated at room temperature for 1 h. Then 20 μL of 75 μM Thioflavine T solution was added, pipette-mixed and immediately submitted for fluorescence measurement (λ_{exc} = 450 nm, λ_{det} = 490 nm). All solutions were prepared in 10 mM PBS at pH 7.4. The fiber content is expressed as percentage in regards to control groups (negative = 0%, positive = 100%). All measurements were done in triplicates and the results averaged.

Insulin aggregation and fibrillation

Samples with appropriate RP concentrations were prepared in 10 mM PBS and the pH adjusted to 7.4. Then, a human insulin stock solution (10 mg mL^{-1}) was added to yield a final protein concentration of 2 mg mL^{-1}. Identical control samples (without protein) were prepared simultaneously and subjected to the same treatment. A total of 2 mL for each solution was transferred to GC vials and submerged in a water bath at 37 °C. Magnetic stirrers inside the vials provided constant agitation (500 rpm). At appropriate time intervals, small aliquots (50 μL) were retrieved and transferred to a (half area) 96 well microplate. Then, absorbance was measured using a Tecan nano M multimode plate reader at 600 nm. After this, 25 μL of a Thio T solution (45 μM in PBS) was added to each vial, pipette-mixed and the fluorescence was measured (λ_{exc} = 450 nm, λ_{det} = 482 nm). All necessary background corrections were made and each sample was measured at least in triplicates and the results averaged.

HPLC

HPLC was performed on a Waters 717plus with a RP-18 column at 30 °C. Detection was done photometrically at λ_{Det} = 310 nm by use of a Waters 2487 unit. HPLC–MS was carried out using an Agilent Q-TOF 6540 UHD. The PR sample was dissolved in water/acetonitrile 98/2 at pH 7.0 in a concentration of 0.2 mg mL^{-1} (for gradient table see Table S1, ESI†).

Fly keeping and incubation

Fly stocks were kept in glass vials containing drosophila standard cornmeal medium and stored in a humid incubator at 18 °C, a relative humidity of 65% and a 12 hour light/dark cycle. In order to overexpress human Aß, Aß40 and Aß42 fly stocks were obtained from the Bloomington Stock Center (numbers 64215 and 64216, respectively) and 2xAß42 as a kind gift from Sergio Casas-Tinto (UAS-Aß42(2x)). UAS-GFP lines (Bloomington Stock number 5431) were used as a control group. The panneuronal Elav-GAL4 line (Bloomington Stock number 458) was combined with temperature sensitive GAL80 protein alleles under the control of a ubiquitous promoter (TubG80ts, Bloomington Stock number 7018) to suppress the expression of toxic amyloid proteins during *Drosophila* development. Here, GAL80 binds to GAL4 and prevents GAL4-mediated transcription activation. At 18 °C, the temperature-sensitive GAL80 protein is stable and active but becomes degraded and inactive at 29 °C. The expression of the UAS-GAL4 system is repressed at 18 °C, but will be reinstated once the flies are shifted to 29 °C.[21] The flies were transferred into

new vials and split into two groups: normal food (nf) and food supplemented with 480 μM of PR (PR). After breeding and hatching at 18 °C, the adult flies were transferred to 29 °C for an incubation period of 10 days. The flies were transferred into new food every 2–3 days. All experiments were carried out with males flies exclusively, except for semiquantitative real time PCR experiments that were performed using female flies. The experiments were conducted several times with independent setups (2–3 replicates) running in parallel. All experiments were performed in compliance with the author's institute's policy on animal use and ethics.

Fly negative geotaxis assay

The locomotor ability was measured by transferring individual flies into clear, graduated plastic pipettes. For this, the flies were temporarily incapacitated with cold temperatures and allowed to recover for 1 h after transfer. By slightly tapping the pipette on a table surface, the flies were relocated to the bottom and prompted to immediately climb upwards (negative geotaxis behavior). A timer was set to 12 seconds and the maximum vertical distance covered was recorded. 10 flies per genotype were measured 3 times. The experiments were conducted in a controlled environment (temperature, humidity, light).

Wholemount immunostaining

10 days-old flies were fixed for 2 h at room temperature in 4% PFA. After washing with PBS twice, the flies were dissected under the binocular and the brains washed thrice with 0.1% PBST. The primary antibody (1 : 100 in 0.5% PBST-10% NGS) was applied over night at 4 °C. Then the brains were washed thrice with 0.1% PBST and the second antibody (1 : 80 in 0.5% PBST-10% NGS) was again applied at 4 °C over night. Then, the brains were washed thrice with 0.1% PBST and mounted with vectashield, sealed with nail polish and stored in the dark at 4 °C until used.

Confocal microscopy and image handling

All samples were scanned on a Leica TCS SP8 confocal microscopy and image acquisition settings were kept constant for every condition. The specimen were excited with a DPSS laser at 561 nm. The fluorescence signal was detected with a HC PL APO 40x/1.30 oil CS2 objective at 565 nm. Images were taken at a resolution of 1024 × 1024 pixels. The brains were scanned in *z*-stacks (1 μm per slice) resulting in 30–35 images per specimen. Subsequent analysis was carried out using the image processing software Fiji 2.0.0.[22] For this, the background was subtracted *via* the rolling ball method (radius = 50 pixels) and maximum projections of fifteen slices were made. The resulting image was again background subtracted and the contrast was adjusted to improve signal quality.

Fly-head Thio T assay

Male flies were fixed as described above. Then, exactly ten heads for each group were manually removed and transferred to exactly 100 μL of PBS in an Eppendorf snap-cap. The heads were homogenized thoroughly using a vortex-mixer. The snap-caps were centrifuged for 5 min at 2000 rpm to remove debris. The 95 μL were retrieved and transferred to a new tube. 505 μL of PBS was added and pipette-mixed. Then, for each group 6 wells of a half area black μclear 96-well plate were filled with 80 μL of solution and the absorbance at 280 nm was measured to adjust for protein content. Subsequently, 20 μL of Thio T stock solution (in PBS, target conc.: 15 μM) or PBS (for background correction) were added into three wells each and pipette mixed. Endpoint fluorescence was then measured (λ_{exc} = 450 nm, λ_{det} = 490 nm, fixed gain). The measurements were carried out on a Tecan Infinite M nano multi-mode plate reader. The triplicates were corrected for protein content and background and the results averaged.

Semiquantitative real time PCR

Total RNA was extracted from 30 female heads using peqGold TriFast reagent (PEQLAB Biotechnologie GMBH, Erlangen, Germany) following manufacturer's instructions. 500 ng mRNA were converted into cDNA using QuantiTect Rev. Transcription Kit (Qiagen GmbH, Hilden, Germany) and then used for qPCR with ORA qPCR Green ROX L Mix (HighQu, Kralchtal, Germany) on a CFX connect™ Real-Time PCR Detection System (Bio-rad, Hercules, California, U.S.). Sequence of primers used is detailed in Table S2 (ESI†). The ribosomal protein 49 (*rp49*) was used as internal control. The results from at least four independent biological replicates were analyzed with the Bio-Rad CFX manager 3.1 software. Gene expression levels were referred to the internal control, the relative quantification was carried out by means of the ΔΔCt method and the results were plotted as relative mRNA expression. Each experiment consisted of 3 independent biological replicates.

Statistical analysis

The data is presented as a mean ± SD ($N = x$), with x being the number of replicates. For the *in vivo* experiments, unpaired data was compared using a two-tailed students *t*-test and statistically significant differences were reported as *: $P \leq 0.05$; **: $P \leq 0.01$; ***: $P \leq 0.001$; and ****: $P \leq 0.0001$ with *ns* meaning statistically not significant (ns: $P > 0.05$)

Results and discussion

The phosphorylated resveratrol (PR), as used in this study, is commercially available as a mixture of sodium salts (*cf.* Fig. 1 for the molecular structures). Using proton and ^{31}P-NMR, the actual composition of the used product was found to be 45.1 wt% RTP, 15.3 wt% RDP, 9.7 wt% RMP and 0.4 wt% *t*-resveratrol. This translates to an average of 2.4 phosphate units per resveratrol structure. The mixture also contained inorganic phosphates (14.8 wt%, 11.5 wt% and 1.8 wt% for mono-, di-, and triphosphate respectively) as byproducts (details can be found in S3–S5, ESI†). As the PR derivatives are very similar in size and solubility characteristics, separation and isolation in reasonable quantities would prove to be a difficult challenge (*cf.* S3, ESI†). For many experiments, this attempt would also be rendered futile, as PR is not stable in *in vivo* conditions and will be hydrolyzed enzymatically to

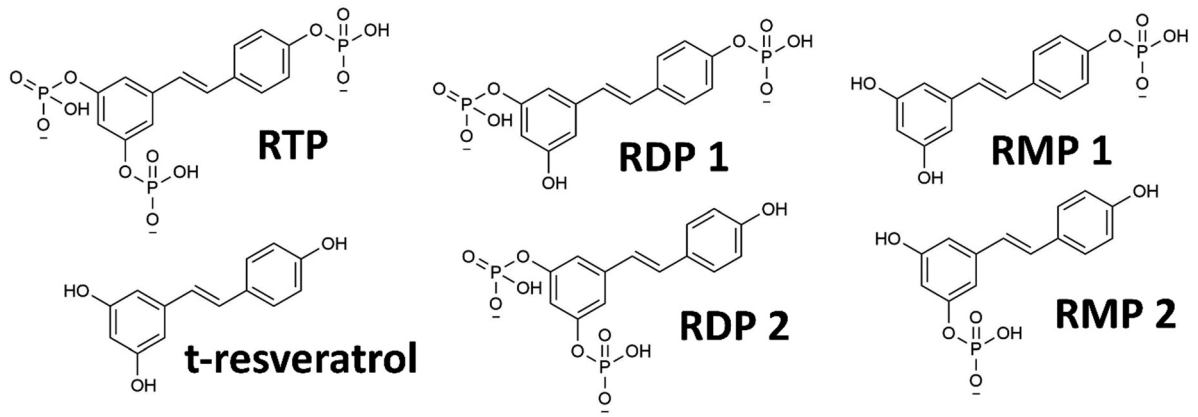

Fig. 1 Molecular structures of various PR derivatives: RTP, RDP and RMP (both with two structural isomers denoted 1 and 2) and the parent compound *trans*-resveratrol.

derivatives with a lower number of phosphate units (or free *t*-resveratrol) anyway.[23,24] Therefore, the compound was treated as a mixture of chemically related substances that, in essence, present a water-soluble form of *t*-resveratrol with potentially augmented characteristics.

Physicochemical effects of PR

In order to examine the properties of the amphiphilic PR compounds, solubilization experiments were performed. It was found that relatively high concentrations of PR (>100 mM) can solubilize the hydrophobic dye disperse red 13 (DR13), see Fig. 2a. This is normally only the case for surfactants (such as SDS) at low or hydrotropes (such as SXS) at high concentrations.[26] The significantly better performance of PR over the common hydrotrope SXS might be related to the similarities in molecular structure between the dye and RP. They both share a stilbene-type backbone, with the DR13 having an azo-group instead of a C–C double bond linking the two rings (*cf.* Fig. 1). Therefore, specific π–π interactions can lead to complex formation making the dye somewhat soluble. This is often referred to as copigmentation.[27] It has been reported in the past that resveratrol can partake in copigmentation and thus contribute to the color of wine.[28] Hence, it is possible that the much more water-soluble phosphorylated derivative can likewise interact with compounds that share certain similarities and in this way facilitate the solubilization of minute yet measurable quantities of DR13. Further proof of this is the incomplete separation of PR compounds during HPLC, leaving mixed peaks that indicate strong interactions between the structural isomers and derivatives with varying phosphate content (see S3, ESI†). This is, however, not to be confused with general hydrotropic solubilization, even though π–π interactions can play a secondary role for hydrotropes as well.[26] Furthermore, it can be assumed that decreasing phosphate content (RTP > RDP > RMP) will contribute significantly to a surface active behavior, as the salting-out characteristics of the phosphate headgroups will decrease, and the ratio of nonpolar surface/ionic headgroup will increase.[29] This is reflected in the surface tension measurements for PR, that show a significant decrease in surface tension at higher concentrations (Fig. 2a). Here, the minor compounds RDP and

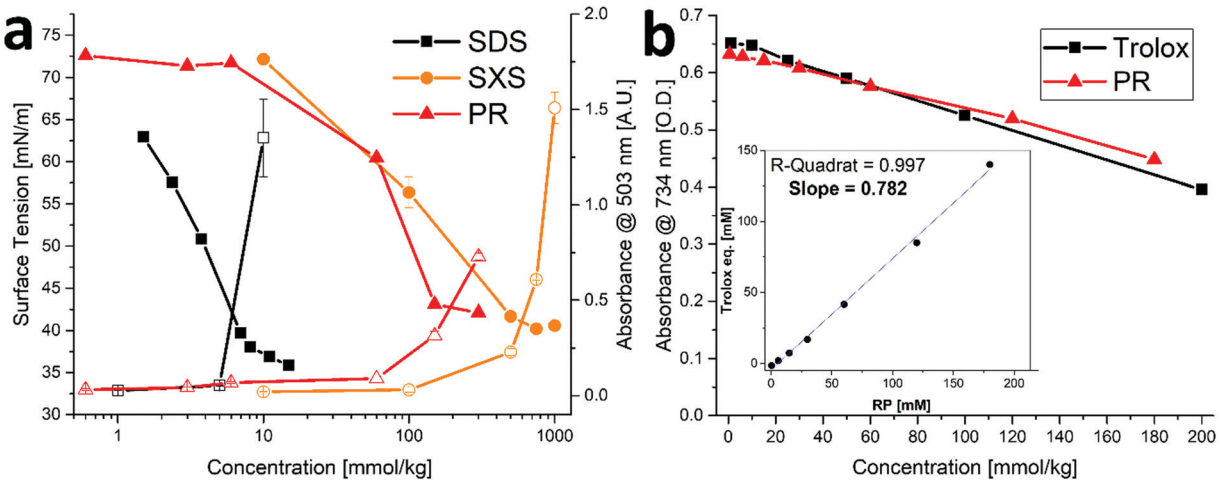

Fig. 2 Physicochemical effects of PR. (a) Left axis: surface tension (filled symbols) and right axis: absorbance as measure of DR13 solubilization (hollow symbols) for SDS, SXS and PR. Error bars mean ± SD (N = 2). Data for SDS and SXS are taken from Mehringer *et al.*[25] (b) Trolox anti-oxidant assay for Trolox and PR. Error bars mean ± SD (N = 2). Insert: Trolox equivalents of PR *vs.* PR concentration yielding the average trolox value as slope.

RMP will be present in significant enough amounts to exhibit a noticeable surface activity. This is likely to contribute significantly to the DR13 solubilization.

Trans-Resveratrol is a known anti-oxidant,[10,11] therefore, it was examined if and to what extent the phosphorylation affects this property. As can be seen in Fig. 2b, the trolox assay (using ABTS) was performed for PR yielding a trolox value of ≈ 0.78. This means that one molecule of PR is about 78% as effective as the reference anti-oxidant trolox. For *trans*-resveratrol, the literature reports a trolox value of approximately 0.33, albeit at a significantly lower concentration regime due to the limited solubility of *trans*-resveratrol.[30] We conclude therefore that the anti-oxidant capacity of PR is not affected by the phosphorylation. Instead, it was reported in the past that modification of the hydroxy-group to make it unavailable (*e.g.* by methylation) can help hinder the degradation of the resveratrol structure, particularly due to photochemical transformations.[31]

Biochemical effects of PR *in vitro*

In this section, the effects of PR on protein aggregation and fibrillation were examined. For this, solutions of diluted crude chicken egg white (CCEW) were heated and the subsequent denaturation followed by aggregation was monitored *via* turbidity measurements. As can be seen in Fig. 3a, increasing concentrations of PR lead to a reduction in turbidity and for 6 mM PR even increased the transmission up to 75 °C until aggregation (presumably of more thermostable ovalbumin) set in. PR could apparently prevent the (partially) unfolded egg white proteins from sticking together to produce a large network, which is usually the principal cause for the observed

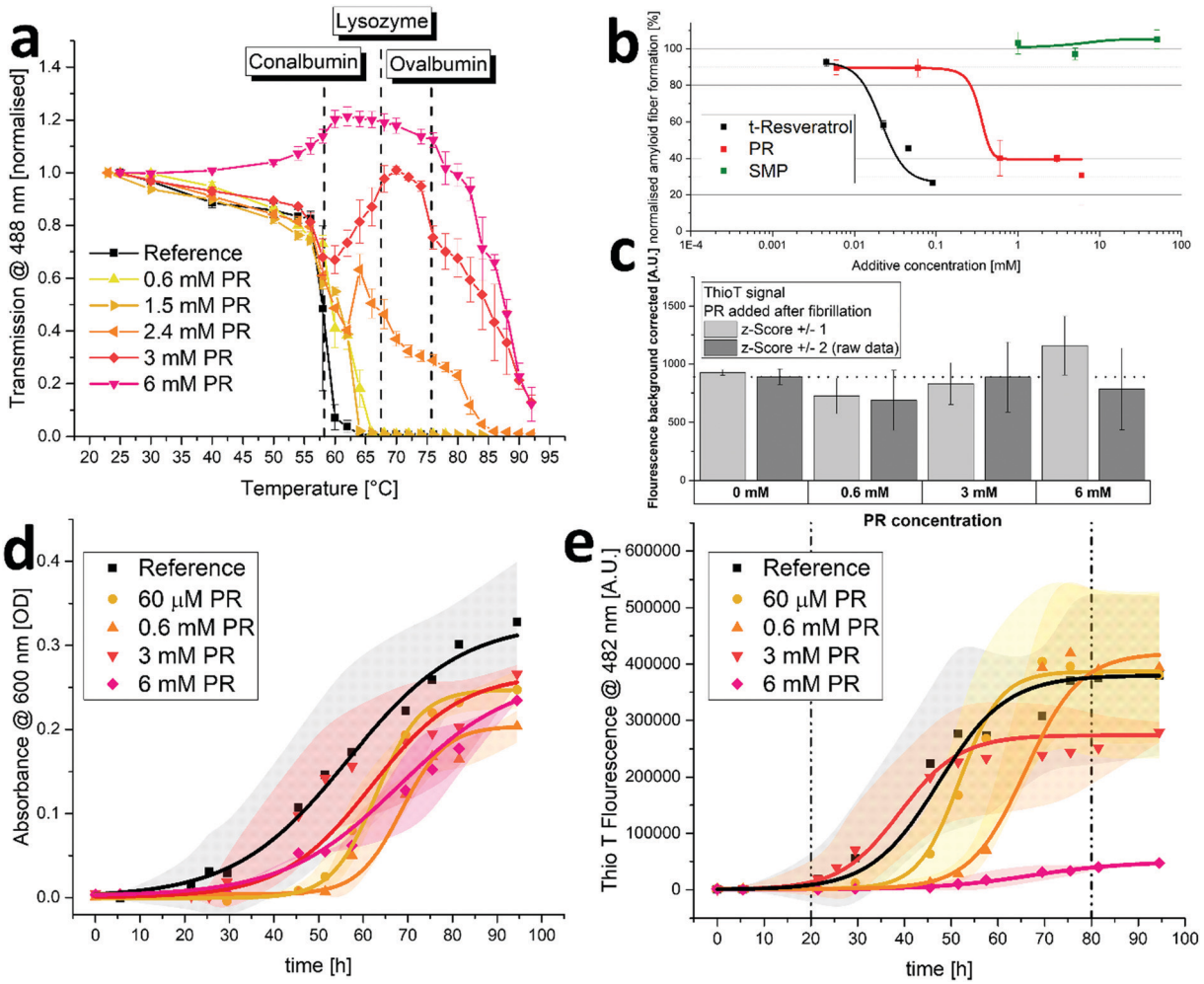

Fig. 3 Biochemical effects of PR *in vitro*. (a) Turbidity of CCEW solutions (pH 7.4) with various PR concentrations as a function of temperature. Error bars mean ± SD (N = 3). Indicated are the approximate denaturation temperatures of the main egg white fractions in CCEW as determined by DSC. (b) Amyloid beta 42 fibrillation with various additives. Measured *via* Thio T staining and normalized according to reference (PBS only). Error bars mean ± SD (N = 3). (c) Thio T fluorescence of amyloid fiber-probe in presence of amyloid beta 42 with PR added after fibrillation to yield different concentrations. Data is represented as raw data (all points abide z-score ±2) and filtered data according to a z-score of ±1. Error bars mean ±SD (N = 3 for raw data). (d and e) Insulin aggregation (d) and fibrillation (e) as measured by turbidity and Thio T fluorescence over time with various PR concentrations. Conditions were 2 mg mL^{-1} human insulin in 10 mM PBS (pH 7.4) at 37 °C with constant agitation. Reference is in buffer only. The shaded areas represent ± SD (Reference: N = 9, 60 µM, 0.6 mM & 6 mM: N = 3, 3 mM: N = 6).

turbidity.[32] While some limited effect on the aggregation is also observed for other ionic compounds (kosmotropic, chaotropic or hydrotropic), this behavior is very unusual and was not seen in this quantity or quality with a variety of other substances (see S6, ESI†).

Next, a specific subspecies of protein aggregation, namely fibrillation, was examined. During fibrillation, susceptible proteins undergo a transformation toward a beta-sheet-rich conformation which will in turn facilitate the aggregation into highly structured fibrils often called amyloid-like. The appearance of these aggregates is associated with a variety of neurodegenerative or conformational diseases such as amyloidosis, Alzheimer's and Parkinson's diseases.[5–7] The intrinsically disordered peptide amyloid beta 42 (Aß42) is known to be very prone to fibrillation and easily forms amyloid type fibers in aqueous environments. The amount of formed fibrillose material can be quantified using the highly specific fluorescent probe Thio T.[33] As can be seen in Fig. 3b, the addition of PR can reduce the amount of formed fibers at concentrations below 1 mM. It was reported in the past that resveratrol is also effective in preventing the fibrillation of amyloidogenic peptides,[15,16] which is also represented in Fig. 3b. Here, it appears that PR is actually less effective than *trans*-resveratrol, as it requires roughly ten times the concentration. It is likely that different PR derivatives have varying efficiencies in preventing fibrillation, including the possibility that some derivatives have little or no efficiency at all. In a previous work by Sciacca *et al.*, the resveratrol monophosphate RMP 1 was shown to be very effective in preventing amyloid growth of human islet amyloid peptide, outperforming *trans*-resveratrol at small concentrations.[34] As the overall effect of PR appears to be weaker than that of free *t*-resveratrol, the remaining constituents in the PR mixture (namely RDP and RTP making up almost 80% of the mixture, *cf.* S5, ESI† a) might potentially be lower in effectiveness. This could indicate the existence of an optimal degree of phosphorylation for anti-fibrillation properties of resveratrol structures.

It was reported in the past that some polyphenolic substances can intervene in fluorescence assays to detect amyloid fibers. Competitive binding with the dye can lead to false positive anti-aggregation activities and additional experiments to exclude this possibilities are advised.[35] Therefore, an Aß42 aggregation assay, akin to what was reported in Fig. 3b, was run in PBS buffer only. Then, after completion of aggregation, PR was added to yield a final concentration that matched the ones used in the actual assay. The results showed little effect of PR additive on the recorded fluorescence signal (see Fig. 3c), indicating no major interference with the assay. This also shows that the formed fibrils are stable and do not dissolve into non-fibrous material upon mixture with PR (with little to no incubation time), which would have resulted in significantly lower fluorescence signals.

Next, the aggregation of human insulin (HI) was examined. It was reported in the past that HI will aggregate and form amyloid-type fibers under a variety of conditions.[36,37] The experiment showed that at physiological conditions (pH 7.4, 37 °C), HI will aggregate during constant agitation after an induction time of roughly 24 hours resulting in increasing turbidity of the solution (see Fig. 3d). Adding varying amounts of PR had only minor diminishing effects on the apparent aggregation. Further evaluation using Thio T fluorescence, however, revealed the effect of PR on fibrillation, as the amount of formed amyloid-type fibers are detected as opposed to the overall amount of aggregation (including amorphous aggregates) using turbidimetry only. As can be seen in Fig. 3e, the fibrillation principally follows a sigmoidal curve for all samples with an induction period of about 1 day and a plateau after 4–5 days, indicating an endpoint to the fibrillation. As can be expected,[38] time resolved experiments are very prone to kinetic effects, resulting in broad standard deviations and the behavior during growth phase (indicated by broken lines) does not strictly correlate with the amount of PR added. However, the endpoint does depend on the PR content, yielding significantly lower fiber fluorescence signals for 3 mM and almost no fluorescence for 6 mM of PR. It should be noted that this experiment is conducted with a relatively high protein load of 2 mg mL^{-1}, which increases fibrillation (both, quantity and kinetics).[36] It also requires higher additive concentrations to achieve additive/protein ratios necessary to inhibit the formation of fibers. While PR cannot prevent the aggregation of HI entirely, it can inhibit the fibrillation. This indicates that PR can steer the aggregation pathway away from amyloid-fibers and toward other, possibly amorphous aggregates. This effect was also previously reported for *trans*-resveratrol on human islet amyloid peptide.[16]

Biochemical effects of PR *in vivo*

The *in vivo* capabilities of PR were examined by using *Drosophila melanogaster* as a model organism. To this effect, genetically modified flies were used to simulate Alzheimer's type amyloid overexpression.[39,40] Two different fly strains were used to provoke Alzheimer's disease phenotypes, carrying either one or two copies of the Aß42 mutant transgene (1xAß42, 2xAß42). As controls, genotypes with an overexpression of an innocuous protein such as green fluorescent protein (GFP) and the overexpression of the wildtype Aß (1xAß40) were included. As Aß42 expression strongly impairs fly development, a temperature sensitive inhibitor gene (TubG80ts) was deployed to allow a healthy development from larvae to fully hatched flies. Fig. 4a shows the effect of temperature incubation in 10 days-old flies when the expression of Aß is blocked at 18 °C and when it is promoted at 29 °C. At the lower temperature, the inhibitor gene is activated and suppresses the expression of Aß42. This results in agile and healthy flies that exhibit normal locomotor performance (*cf.* GFP flies at 29 °C in Fig. 4b as healthy controls). Transgenic Aß flies that were incubated at 29 °C on the other hand exhibited severe locomotive impairment, with a reduction of around 60% in their climbing speeds. To assess if the PR-supplementation can counteract the neurological manifestations of Aß42 overexpression, flies were grown and aged (at 29 °C for 10 days) in fly food that was supplemented with 480 μM of PR *versus* an untreated control group (nf). The results for various genotypes can be seen in Fig. 4b: here,

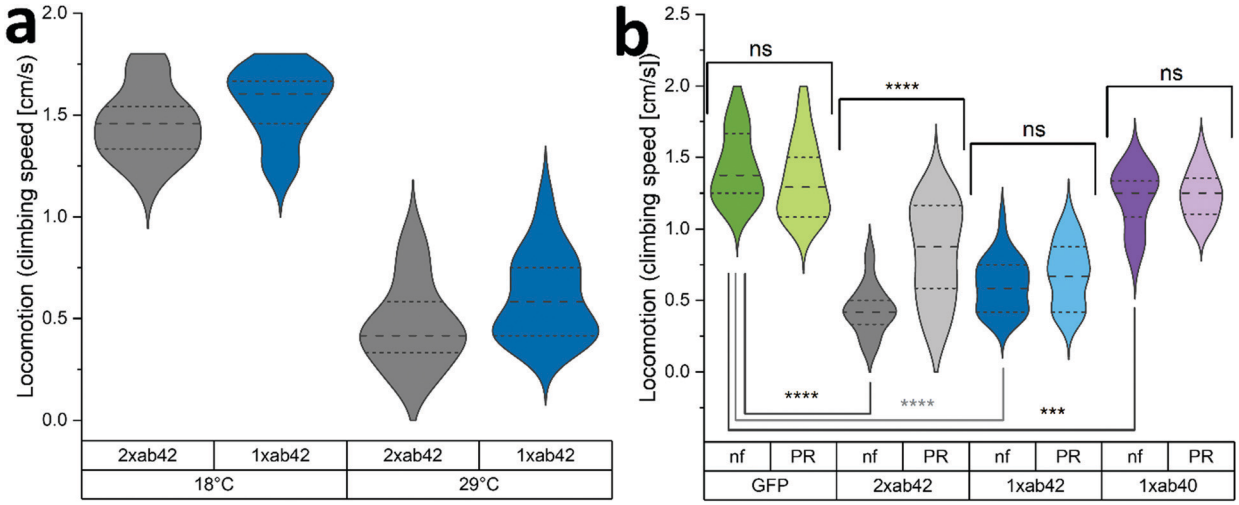

Fig. 4 Negative geotaxis assay of flies overexpressing control and toxic forms of amyloid protein. (a) Locomotion data for amyloid flies kept at 18 °C or 29 °C for 10 days (N = 18). (b) Climbing speed for various genotypes after 10 days at 29 °C (N = 24–30). nf groups have been fed with normal food, PR groups have been fed with PR spiked (480 μM) fly food during development and aging. Comparison between groups with students t-test (*: $P \leq 0.05$; **: $P \leq 0.01$; ***: $P \leq 0.001$; and ****: $P \leq 0.0001$ with ns meaning statistically not significant (ns: $P > 0.05$).).

GFP flies served as a "genetically healthy" reference setting the climbing speed benchmark. While the locomotive impairment is substantial for 1xAß42 and 2xAß42 genotypes, Aß40 flies exhibited only a slight reduction in agility (≈15%), as this amyloid subtype is less aggregation-prone and neurotoxic.[41,42] Importantly, for the most affected 2xAß42 flies, a significant difference among the food groups was detected: for this genotype a notably better retention of locomotor abilities was observed in the PR fed group, suggesting a physiological effect of the additive.

In order to test whether the correlation of physical fitness and supplementation with PR might be caused by an effect of the additive on the expression levels of Aß42, we decided to monitor the corresponding transcription levels. Fig. 5a shows relatively uniform RNA levels for both food groups, giving no indication for a gene-regulating effect. Next, the influence of PR on the accumulation of Aß42 protein in the fly brains was investigated by confocal microscopy. To better understand the cellular mechanisms underlying the improvement of the locomotor abilities, we further analysed the conformational situation of Aß42 protein using three different antibodies targeting the sequence or morphology (oligomer or fiber) of Aß42. As can be seen in Fig. 5b, whole-mount immunostaining using a sequence specific antibody revealed a clear reduction in Aß42 levels, for both genotypes examined (1xAß42 & 2xAß42). The confocal microscopy images in Fig. 5c are representative for nf (untreated) and PR food groups. The detected signal, however, does not differentiate between Aß42 conformers (fibre, oligomer, amorphous), which are known to vary greatly in neurotoxicity.[43] Therefore, aggregation specific antibodies were deployed next to further investigate the effect of PR. For this, homogenized fly head extracts were measured with the fluorescent Thio T dye (*cf.* previous section). As can be seen in Fig. 5d, the strength of the fluorescent signal was dependent on both, the amount of Aß42 gene copies as well as the food group. It showed that samples prepared from PR fed flies exhibited a significantly lower Thio T fluorescence, indicating a reduced amount of amyloid fibres.[44] In additional experiments, whole-mount immunostaining with aggregation specific antibodies was used to elucidate the aggregation state for 2xAß42 genotype flies (see Fig. 5e and Fig. S7, ESI†). The staining with the oligo-specific antibody (A11) exhibited no statistically significant difference across the two food groups. For the fiber-specific immunostaining, the PR food group individuals showed a significantly increased fluorescence. A previous study on drosophila Aß42 models related higher fiber content with better physical fitness, as this appears to be the less neurotoxic morphology compared to oligomers or pre-fibrillar states.[45] While this appears to disagree with the Thio T results (see Fig. 5d), one must take into account that according to the manufacturer, the antibody (AB2286) does not exclusively bind to fibrils but also to a lesser extent to Aß42 monomers. Furthermore, fibril OC antibodies were found to be rather selective for specific fiber polymorphisms revealing varying binding affinities.[46]

While the exact mechanism remains unclear, the reduced amounts of Aß42 protein (Fig. 5b) could be related to a modulating effect on aggregation morphology (Fig. 5d and e) and an improved peptide clearance.[42,45] Both would result in a reduced neurotoxicity, explaining the improved locomotive abilities (Fig. 4b) for PR supplemented flies.

Conclusions

The PR compounds are an interesting set of molecules that show a variety of effects that have their roots in multiple pathways (see Fig. 6). As it became apparent in Fig. 2b, PR retains the anti-oxidant behavior known for the free t-resveratrol compound. A previous dietary study with RTP showed a significant reduction of oxidative stress *in vivo*.[47] This

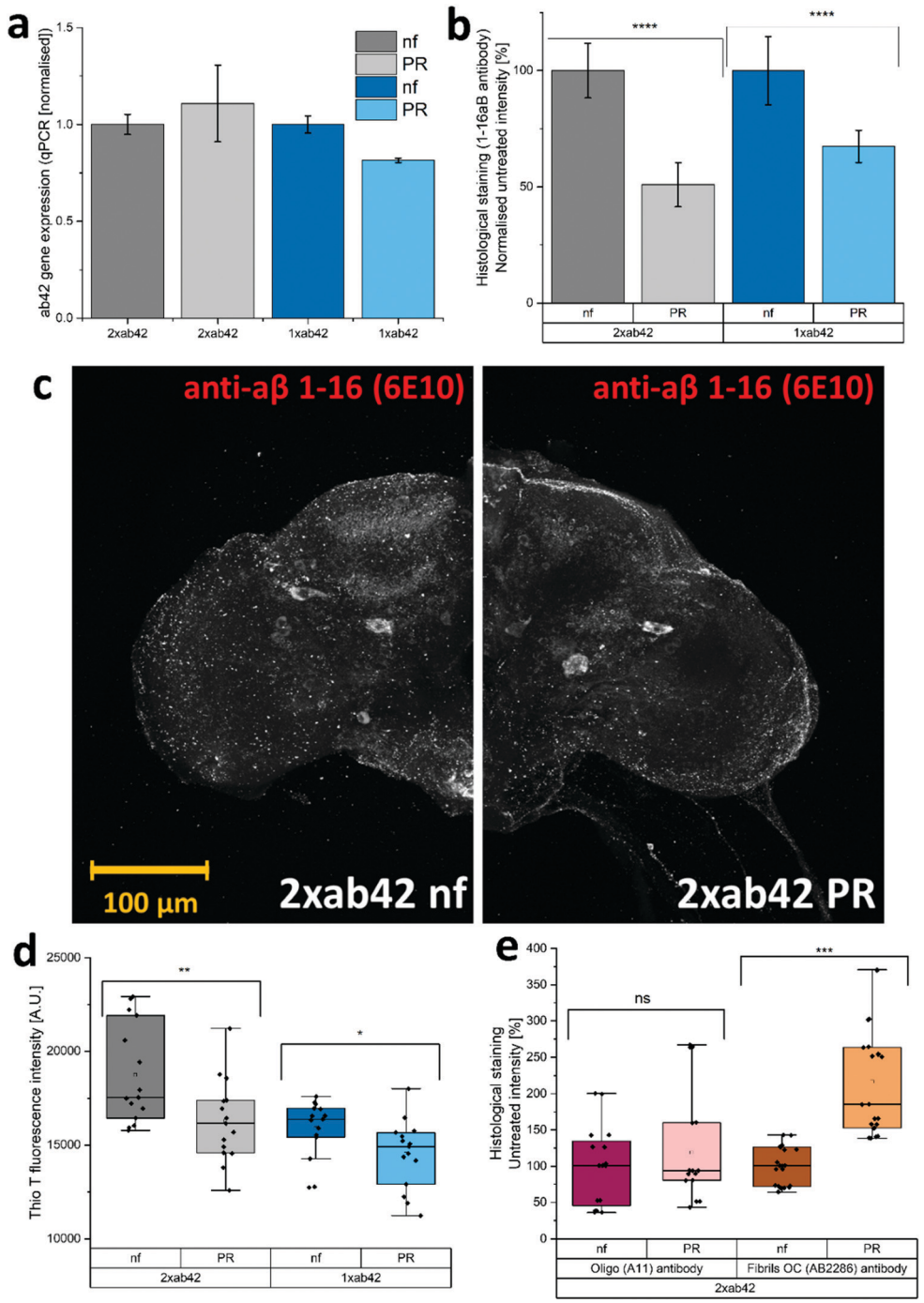

Fig. 5 (a) Aß42 gene expression as measured by qPCR. Data was collected in two independent experiment and qPCR runs and the results averaged. (b) Integrated density of the fluorescence signal for a sequence specific Aß42-antibody (1-16ab). For each group 10–12 brains were analysed using confocal microscopy. The brains for each group were gathered in 4 independent experiments. (c) Confocal microscopy pictures (max. intensity projection) of drosophila brains exemplifying the difference in sequence specific antibody binding between the two food groups. (d) Thio T fluorescence of homogenized fly-head extracts. The box plot shows data gathered in 5 separate experiments ($N = 5 \times 10$). (e) Integrated density of the fluorescence signal for aggregation-specific Aß42-antibodies (oligomer & fiber). The data was gathered in 3 separate experiments. For each group at least 5 brains were analysed using confocal microscopy ($N = 3 \times 5$–7). (a–e) Comparison between groups with students t-test (*: $P \leq 0.05$; **: $P \leq 0.01$; ***: $P \leq 0.001$; and ****: $P \leq 0.0001$ with ns meaning statistically not significant (ns: $P > 0.05$).)

was, in part, also attributed to gene regulatory effects of RTP. A property that has also been reported for t-resveratrol.[12,13] Besides this, PR also exhibited potent anti-fibrillation characteristics *in vitro* (*cf.* Fig. 3), which potentially relies on π–π interactions as reported for t-resveratrol.[17] This property also extended into *in vivo* experiments using drosophila as a model organism (*cf.* Fig. 4 and 5). Here, the aggregation of Aß42 could be significantly reduced, resulting in better locomotor

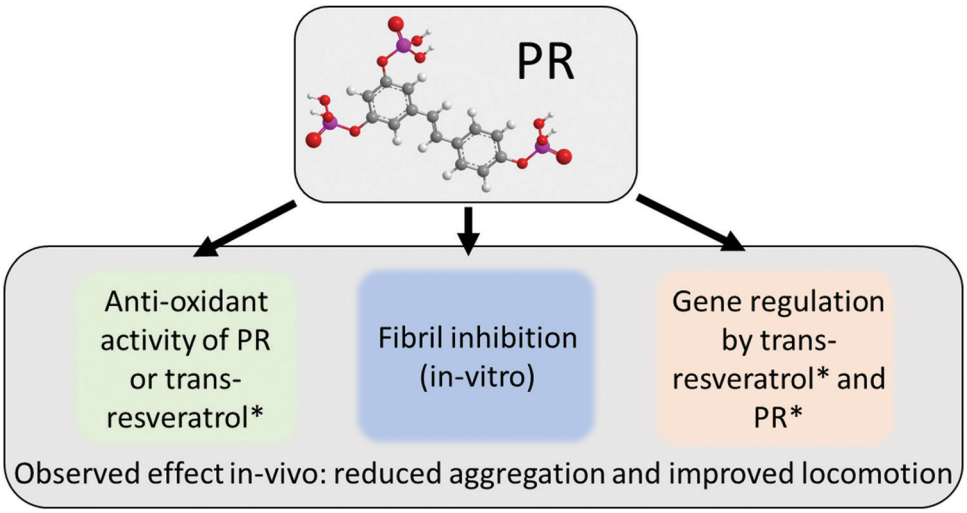

Fig. 6 Scheme summarizing various mechanistic pathways of PR as a direct active or potential prodrug for *in vivo* formation of *trans*-resveratrol. Aspects marked with an asterisk were not the subject of this publication but can be found elsewhere in the works cited in this manuscript.

abilities suggesting a neuroprotective effect. Similar results showing a clear correlation between *in vitro* experiments and *in vivo* drosophila models of Aß42 were reported in the past for compounds such as curcumin and doxycycline.[42,45] It was suggested previously that PR has an improved bioavailability over *t*-resveratrol due to its much higher water-solubility.[9] Aleo *et al.*, however, also reported different biological activities for various PR derivatives, which might be connected to different membrane interaction characteristics.[48,49] This unresolved discussion was circumvented by deploying a whole host of different PR compounds at once, but could and should be the target of a future inquiry. This way, PR could also be considered as a potential prodrug for individual degradation products (*cf.* Fig. 1), as phosphate groups are gradually cleaved off *in vivo*. The authors are aware that PR derivatives might qualify as pan-assay interference compounds (PAINS), as is the case for *t*-resveratrol.[50,51] While an adverse effect on some assays cannot be excluded, the wealth of previously reported data and the results of this work justify a genuine optimism regarding the present findings. In particular the indirect effects of nutritionally supplemented PR on physiological changes as detected in *in vivo* experiments will be difficult to invalidate with known interference patterns of PAINS.

As mentioned, phosphorylation can yield an improved bioavailability of polyphenols over poorly soluble parent compounds.[20] This was recently demonstrated also for quercetin, where sequential phosphorylation greatly enhanced the water solubility, paving the way for biological studies of this otherwise insoluble polyphenol.[52] Additionally, phosphate moieties might contribute to the anti-aggregation efficacy by bringing in highly charged groups that facilitate electrostatic repulsion in intra- and intermolecular interactions between aggregating proteins. Furthermore, aggregation can also be suppressed by an increase of protein stability. This in turn might be achieved by phosphorylated polyphenols *via* an excluded volume effect, as was previously reported for ATP.[25]

In conclusion, PR could prevent the aggregation of CCEW and the fibrillation of Aß42 and insulin *in vitro*. Additional drosophila fly models also exhibited significant effects, leading to reduced Aß42 aggregation *in vivo* and improved locomotion behaviour (neuroprotection). As the amyloid model in drosophila does not represent the full scope of the Alzheimer's disease, further studies are necessary to evaluate a potential application of PR in pharma.

Author contributions

J. M. conducted the investigation and J. N. helped with the formal analysis. The original draft was written by J. M. and J. N. D. T., W. K. and S. S. contributed to the conceptualization and reviewing of the manuscript.

Conflicts of interest

There are no conflicts to declare.

Acknowledgements

We would like to express our sincere gratitude toward Patrick Ricquier at Ajinomoto OmniChem for providing us with the phosphorylated resveratrol as a free sample. We also like to thank Gudrun Karch at the Institute of Zoology (University of Regensburg) for technical advice with the *Drosophila in vivo* experiments.

Notes and references

1 F. U. Hartl, A. Bracher and M. Hayer-Hartl, Molecular chaperones in protein folding and proteostasis, *Nature*, 2011, **475**, 324–332.
2 F. E. Cohen and J. W. Kelly, Therapeutic approaches to protein-misfolding diseases, *Nature*, 2003, **426**, 905–909.

3 W. Wang, S. Nema and D. Teagarden, Protein aggregation-Pathways and influencing factors, *Int. J. Pharm.*, 2010, **390**(2), 89–99.
4 E. Y. Chi, S. Krishnan, T. W. Randolph and J. F. Carpenter, Physical stability of proteins in aqueous solution: mechanism and driving forces in nonnative protein aggregation, *Pharm. Res.*, 2003, **20**(9), 1325–1336.
5 M. F. Avila-Vazquez, N. F. Altamirano-Bustamante and M. M. Altamirano-Bustamante, Amyloid biomarkers in conformational diseases at face value: a systematic review, *Molecules*, 2018, **23**(1), 1–29.
6 C. Soto and S. Pritzkow, Protein misfolding, aggregation, and conformational strains in neurodegenerative diseases, *Nat. Neurosci.*, 2018, **21**(10), 1332–1340.
7 S. Sheikh, Safia, E. Haque and S. S. Mir, Neurodegenerative Diseases: multifactorial Conformational Diseases and Their Therapeutic Interventions, *J. Neurodegener. Dis.*, 2013, **2013**, 1–8.
8 V. H. Finder, Alzheimer's disease: a general introduction and pathomechanism, *J. Alzheimer's Dis.*, 2010, **22**, S3-19.
9 A. P. Singh, R. Singh, S. S. Verma, V. Rai, C. H. Kaschula and P. Maiti, *et al.*, Health benefits of resveratrol: evidence from clinical studies, *Med. Res. Rev.*, 2019, **39**(5), 1851–1891.
10 F. Caruso, J. Tanski, A. Villegas-Estrada and M. Rossi, Structural basis for antioxidant activity of *trans*-resveratrol: *ab initio* calculations and crystal and molecular structure, *J. Agric. Food Chem.*, 2004, **52**(24), 7279–7285.
11 R. Mikstacka, A. M. Rimando and E. Ignatowicz, Antioxidant effect of *trans*-resveratrol, pterostilbene, quercetin and their combinations in human erythrocytes *in vitro*, *Plant Foods Hum. Nutr.*, 2010, **65**(1), 57–63.
12 Y. Hu, S. Rahlfs, V. Mersch-Sundermann and K. Becker, Resveratrol modulates mRNA transcripts of genes related to redox metabolism and cell proliferation in non-small-cell lung carcinoma cells, *Biol. Chem.*, 2007, **388**(2), 207–219.
13 E. L. Robb, M. M. Page, B. E. Wiens and J. A. Stuart, Molecular mechanisms of oxidative stress resistance induced by resveratrol: specific and progressive induction of MnSOD, *Biochem. Biophys. Res. Commun.*, 2008, **367**(2), 406–412.
14 M. Stefani and S. Rigacci, Protein folding and aggregation into amyloid: the interference by natural phenolic compounds, *Int. J. Mol. Sci.*, 2013, **14**(6), 12411–12457.
15 D. Radovan, N. Opitz and R. Winter, Fluorescence microscopy studies on islet amyloid polypeptide fibrillation at heterogeneous and cellular membrane interfaces and its inhibition by resveratrol, *FEBS Lett.*, 2009, **583**(9), 1439–1445.
16 Y. Feng, X. P. Wang, S. G. Yang, Y. J. Wang, X. Zhang and X. T. Du, *et al.*, Resveratrol inhibits beta-amyloid oligomeric cytotoxicity but does not prevent oligomer formation, *Neurotoxicology*, 2009, **30**(6), 986–995.
17 P. Jiang, W. Li, J. E. Shea and Y. Mu, Resveratrol inhibits the formation of multiple-layered β-sheet oligomers of the human islet amyloid polypeptide segment 22–27, *Biophys. J.*, 2011, **100**(6), 1550–1558.
18 L. Camont, C. H. Cottart, Y. Rhayem, V. Nivet-Antoine, R. Djelidi and F. Collin, *et al.*, Simple spectrophotometric assessment of the *trans*-/*cis*-resveratrol ratio in aqueous solutions, *Anal. Chim. Acta*, 2009, **634**(1), 121–128.
19 V. Vingtdeux, U. Dreses-Werringloer, H. Zhao, P. Davies and P. Marambaud, Therapeutic potential of resveratrol in Alzheimer's disease, *BMC Neurosci.*, 2008, **9**, 1–5.
20 S. Intagliata, M. N. Modica, L. M. Santagati and L. Montenegro, Strategies to improve resveratrol systemic and topical bioavailability: an update, *Antioxidants*, 2019, **8**(8), 244.
21 S. E. McGuire, G. Roman and R. L. Davis, Gene expression systems in Drosophila: a synthesis of time and space, *Trends Genet.*, 2004, **20**(8), 384–391.
22 J. Schindelin, I. Arganda-Carreras, E. Frise, V. Kaynig, M. Longair and T. Pietzsch, *et al.*, Fiji: an open-source platform for biological-image analysis, *Nat. Methods*, 2012, **9**(7), 676–682.
23 G. Zhang, C. R. Flach and R. Mendelsohn, Tracking the dephosphorylation of resveratrol triphosphate in skin by confocal Raman microscopy, *J. Controlled Release*, 2007, **123**(2), 141–147.
24 L. Declercq, H. Corstjens, W. van Brussel and G. Schelkens, *Topical compositions containing phopshorylated polyphenols*, US 8465973 B2, 2013.
25 J. Mehringer, T. Do, D. Touraud, M. Hohenschutz, A. Khoshsima and D. Horinek, *et al.*, Hofmeister versus Neuberg: is ATP really a biological hydrotrope?, *Cell Rep. Phys. Sci.*, 2021, **2**, 100343.
26 P. Bauduin, A. Renoncourt, A. Kopf, D. Touraud and W. Kunz, Unified concept of solubilization in water by hydrotropes and cosolvents, *Langmuir*, 2005, **21**(15), 6769–6775.
27 P. Trouillas, J. C. Sancho-García, V. De Freitas, J. Gierschner, M. Otyepka and O. Dangles, Stabilizing and Modulating Color by Copigmentation: Insights from Theory and Experiment, *Chem. Rev.*, 2016, **116**(9), 4937–4982.
28 J. Heras-Roger, O. Alonso-Alonso, A. Gallo-Montesdeoca, C. Díaz-Romero and J. Darias-Martín, Influence of copigmentation and phenolic composition on wine color, *J. Food Sci. Technol.*, 2016, **53**(6), 2540–2547.
29 J. Mehringer, E. Hofmann, D. Touraud, S. Koltzenburg, M. Kellermeier and W. Kunz, Salting-in and salting-out effects of short amphiphilic molecules: a balance between specific ion effects and hydrophobicity, *Phys. Chem. Chem. Phys.*, 2021, **23**, 1381–1391.
30 C. Lucas-Abellán, M. T. Mercader-Ros, M. P. Zafrilla, J. A. Gabaldón and E. Núñez-Delicado, Comparative study of different methods to measure antioxidant activity of resveratrol in the presence of cyclodextrins, *Food Chem. Toxicol.*, 2011, **49**(6), 1255–1260.
31 I. Yang, E. Kim, J. Kang, H. Han, S. Sul and S. B. Park, *et al.*, Photochemical generation of a new, highly fluorescent compound from non-fluorescent resveratrol, *Chem. Commun.*, 2012, **48**(32), 3839–3841.
32 A. Handa, K. Takahashi, N. Kuroda and G. W. Froning, Heat-induced egg white gels as affected by pH, *J. Food Sci.*, 1998, **63**(3), 403–407.

33 H. LeVine III, Quantification of β-sheet amyloid fibril structures with thioflavin T, *Methods Enzymol.*, 1999, **309**, 274–284.
34 M. F. M. Sciacca, R. Chillemi, S. Sciuto, V. Greco, C. Messineo and S. A. Kotler, *et al.*, A blend of two resveratrol derivatives abolishes hIAPP amyloid growth and membrane damage, *Biochim. Biophys. Acta, Biomembr.*, 2018, **1860**(9), 1793–1802.
35 L. P. Jameson, N. W. Smith and S. V. Dzyuba, Dye-binding assays for evaluation of the effects of small molecule inhibitors on amyloid (Aβ) self-assembly, *ACS Chem. Neurosci.*, 2012, **3**(11), 807–819.
36 L. Nielsen, R. Khurana, A. Coats, S. Frokjaer, J. Brange and S. Vyas, *et al.*, Effect of environmental factors on the kinetics of insulin fibril formation: elucidation of the molecular mechanism, *Biochemistry*, 2001, **40**(20), 6036–6046.
37 S. H. Wang, X. Y. Dong and Y. Sun, Effect of (−)-epigallocatechin-3-gallate on human insulin fibrillation/aggregation kinetics, *Biochem. Eng. J.*, 2012, **63**, 38–49.
38 L. Giehm, N. Lorenzen and D. E. Otzen, Assays for α-synuclein aggregation, *Methods*, 2011, **53**(3), 295–305.
39 K. Iijima, H. P. Liu, A. S. Chiang, S. A. Hearn, M. Konsolaki and Y. Zhong, Dissecting the pathological effects of human Aβ40 and Aβ42 in Drosophila: a potential model for Alzheimer's disease, *Proc. Natl. Acad. Sci. U. S. A.*, 2004, **101**(17), 6623–6628.
40 R. Chakraborty, V. Vepuri, S. D. Mhatre, B. E. Paddock, S. Miller and S. J. Michelson, *et al.*, Characterization of a drosophila Alzheimer's disease model: pharmacological rescue of cognitive defects, *PLoS One*, 2011, **6**, 6.
41 T. Harada and R. C. D. Kuroda, Measurements of β-amyloid (1-40) and (1-42) in the condensed phase, *Biopolymers*, 2011, **95**(2), 127–134.
42 R. Costa, E. Speretta, D. C. Crowther and I. Cardoso, Testing the therapeutic potential of doxycycline in a Drosophila melanogaster model of Alzheimer disease, *J. Biol. Chem.*, 2011, **286**(48), 41647–41655.
43 K. Broersen, F. Rousseau and J. Schymkowitz, The culprit behind amyloid beta peptide related neurotoxicity in Alzheimer's disease: oligomer size or conformation?, *Alzheimer's Res. Ther.*, 2010, **2**(4), 12.
44 O. V. Nevzglyadova, E. V. Mikhailova, T. R. Amen, V. V. Zenin, A. V. Artemov and E. I. Kostyleva, *et al.*, Yeast red pigment modifies Amyloid beta growth in Alzheimer disease models in both Saccharomyces cerevisiae and Drosophila melanogaster, *Amyloid*, 2015, **22**(2), 100–111.
45 I. Caesar, M. Jonson, K. P. R. Nilsson, S. Thor and P. Hammarström, Curcumin promotes a-beta fibrillation and reduces neurotoxicity in transgenic Drosophila, *PLoS One*, 2012, **7**(2), e31424.
46 A. Hatami, R. Albay, S. Monjazeb, S. Milton and C. Glabe, Monoclonal antibodies against Aβ42 fibrils distinguish multiple aggregation state polymorphisms *in vitro* and in Alzheimer disease brain, *J. Biol. Chem.*, 2014, **289**(46), 32131–32143.
47 D. De Groote, K. Van Belleghem, J. Devire, W. Van Brussel, A. Mukaneza and L. Amininejad, Effect of the intake of resveratrol, resveratrol phosphate, and catechin-rich grape seed extract on markers of oxidative stress and gene expression in adult obese subjects, *Ann. Nutr. Metab.*, 2012, **61**(1), 15–24.
48 D. Aleo, V. Cardile, R. Chillemi, G. Granata and S. Sciuto, Chemoenzymatic Synthesis and Some Biological Properties of *O*-phosphoryl Derivatives of (*E*)-resveratrol, *Nat. Prod. Commun.*, 2008, **3**(10), 1693–1700.
49 M. F. M. Sciacca, R. Chillemi, S. Sciuto, M. Pappalardo, C. La Rosa and D. Grasso, *et al.*, Interactions of two *O*-phosphoryl-resveratrol derivatives with model membranes, *Arch. Biochem. Biophys.*, 2012, **521**(1–2), 111–116.
50 J. L. dos Santos, Pan-Assay Interference Compounds (PAINS): Warning Signs in Biochemical-Pharmacological Evaluations, *Biochem. Pharmacol.*, 2015, **04**, 02.
51 J. B. Baell, Feeling Nature's PAINS: Natural Products, Natural Product Drugs, and Pan Assay Interference Compounds (PAINS), *J. Nat. Prod.*, 2016, **79**(3), 616–628.
52 F. J. Osonga, J. O. Onyango, S. K. Mwilu, N. M. Noah, J. Schulte and M. An, *et al.*, Synthesis and characterization of novel flavonoid derivatives *via* sequential phosphorylation of quercetin, *Tetrahedron Lett.*, 2017, **58**(15), 1474–1479.